Int J Clin Exp Pathol 2019;12(6):2022-2033
www.ijcep.com /ISSN:1936-2625/IJCEP0093024

Original Article

Long non-coding RNA HEIH contributes to diabetic retinopathy by regulating miR-939/VEGF axis

Chengyuan Zhao, Xiaoqiang Fei, Bangkui Xu, Yu Lu, Qingqing Zhang

Department of Endocrinology, Taizhou People's Hospital, Taizhou, Jiangsu, China

Received February 25, 2019; Accepted April 19, 2019; Epub June 1, 2019; Published June 15, 2019

Abstract: Diabetes is one of the most prevalent metabolic diseases in the world. This study explored the role of long non-coding RNA HEIH in regulating the development of diabetic retinopathy (DR). The expression of HEIH gene was detected in the serum of patients with DR. Subsequently, high concentrations of D-glucose (HG) were used to stimulate ARPE-19 cells to construct a cell model of DR. HEIH was overexpressed and suppressed to further investigate the effects of HEIH on HG-induced ARPE-19 cell injury. Moreover, the regulatory relationship between HEIH and miR-939 was investigated, and a target relationship between miR-939 and VEGF in ARPE-19 cells was explored. We elucidated an association between HEIH/miR-939/VEGF axis and the PI3K/AKT pathway. HEIH was highly expressed in the serum of patients with DR. Moreover, HG-induced ARPE-19 cell injury and expression of HEIH. The overexpression of HEIE aggravated HG-induced ARPE-19 cell injury by significantly inhibiting cell viability, inducing apoptosis, promoting cytochrome C release from mitochondria to cytoplasm, and enhancing the caspase-3 activity, whereas suppression of HEIE had the opposite effects. In addition, the effects of the suppression of HEIH on HG-induced ARPE-19 cell injury were markedly reversed by inhibiting miR-939. miR-939 regulated HG-induced ARPE-19 cell injury by targeting VEGF. The suppression of HEIH reversed HG-induced activation of the PI3K/AKT signaling pathway. Our findings revealed that HEIH may contribute to DR by sponging miR-939 to target VEGF expression and by regulating the activation of the PI3K/AKT pathway. Inhibition of epidermal growth factor receptor and PI3K/Akt signaling suppresses cell proliferation and survival through regulation of Stat3 activation in human cutaneous squamous cell carcinoma. HEIH/miR-939/VEGF axis may provide a novel perspective for DR therapy.

Keywords: Diabetic retinopathy, long non-coding RNA, HEIH, miR-939, vascular endothelial growth factor

Introduction

Diabetes is one of the most common metabolic diseases worldwide [1]. The global prevalence of diabetes and associated mortality are continuously increasing with the rise in the living standards [2]. Diabetic retinopathy (DR) is a chronic complication of diabetes caused by long-term hyperglycemia [3, 4]. It is characterized by an early loss of capillary pericytes and thickening of the basement membrane [5]. The disease condition improves in almost 90% of DR patients after appropriate treatment; however, it leads to blindness in the remaining 10% for unexplained reasons [6]. In order to improve the clinical outcome of DR patients, it is crucial to deepen understanding of the key mechanism of this disease.

Long non-coding RNAs (lncRNAs), longer than 200 nucleotides, have gained interest due to their role in diverse biological and physiologic processes [7-9]. Increasing studies have highlighted that the aberrant expression of lncRNAs leads to DR. Many studies have shown that the overexpression of lncRNA H19 prevents glucose-induced endothelial-mesenchymal transition in DR [10]; overexpression of maternally expressed gene 3 suppresses DR development by regulating transforming growth factor beta 1 (TGFβ1) and vascular endothelial growth factor (VEGF) [11]; and nuclear paraspeckle assembly transcript 1 inhibits the apoptosis of retinal Müller cells after DR by modulating the miR-497/brain-derived neurotrophic factor axis [12]. However, the key lncRNAs involved in DR have not been fully identified. Recently, HEIH was identified as an oncogenic lncRNA that promoted tumor progression in hepatocellular carcinoma [13] and colorectal cancer [14]. However, there is no study reporting the association between HEIH and DR.

In this study, we first analyzed the expression of HEIH in clinical serum samples of patients with DR. Subsequently, we stimulated ARPE-19 cells using a high concentration of D-glucose (HG) to construct a cell culture model of DR. HEIH was overexpressed and suppressed to investigate the effects of HEIH on HG-induced ARPE-19 cell injury. It has been reported that lncRNAs function as competitively endogenous RNAs (ceRNAs) to regulate mRNAs, thus regulating the development of human diseases [15]. Therefore, we investigated the regulatory relationship between HEIH and miR-939, and explored a target relationship between miR-939 and VEGF in ARPE-19 cells. We elucidated the role of the PI3K/AKT pathway in regulating HG-induced ARPE-19 cell injury by the HEIH/miR-939/VEGF axis. Our findings will lay a theoretical basis to understand molecular mechanisms underlying DR.

Materials and methods

Patients

The participants were consecutively selected between April 2016 and April 2018 and included 36 healthy participants (healthy control (HC) group), 36 type 1 diabetes (T1D) patients without DR (NDR group), and 36 T1D patients with DR (DR group). Patients with hepatic insufficiency, cardio-cerebrovascular events, renal impairment, pregnancy and postpartum in the previous three months, with infectious diseases, or other severe systemic diseases were excluded. Anthropometric and biochemical assessments were performed using standardized protocols. Moreover, ophthalmologic examinations, including visual function and changes in ocular anterior and posterior segments, were conducted in all individuals. Peripheral venous blood was taken and serum samples were collected, aliquoted into RNase-free microcentrifuge tubes, and stored at -80°C. This study was approved by the ethics committee of our hospital and followed the Declaration of Helsinki. All individuals signed written informed consent before the enrollment.

Cell culture and treatment

The human retinal pigment epithelial cell line ARPE-19 was obtained from the American Type Culture Collection (ATCC) (Manassas, VA, USA). ARPE-19 cells were seeded in 24-well plates at a density of 2.0×10^4 cells/well and maintained with DMEM/F12 conditioned medium containing 10% FBS and penicillin-streptomycin (100 U/mL and 100 μg/mL) in a 37°C incubator with 5% CO_2. The cells were incubated with normal concentration of D-glucose (5 mmol/L; Sigma-Aldrich, St. Louis, MO, USA) for four days, and then exposed to either a normal concentration of D-glucose (5 mmol/L, control) or high concentration of D-glucose (30 mmol/L, HG) for another 48 h.

Cell transfection

To overexpress and suppress HEIH, ARPE-19 cells were transfected with pcDNA-HEIH and si-HEIH, respectively, using Lipofectamine 2000 (Invitrogen, California, USA) according to the manufacturer's instructions. Additionally, ARPE-19 cells were transfected with miR-939 mimic, mimic NC, inhibitor NC, miR-939 inhibitor, pEX, pEX-VEGF, sh-NC, or sh-VEGF using the same method.

Cell viability assay

The viability of ARPE-19 cells was determined by a 3-(4,5-dimethylthiazol-2-yl)-2,5 diphenyl tetrazolium bromide (MTT; Sigma-Aldrich) assay after the treatment. The cells were seeded in 96-well plates at a density of 3.0×10^3 cells/well and exposed to different treatments for 24 h. MTT solution (0.5 mg/mL; 100 μL) was added to each well and incubated for 4 h at 37°C. After removing the MTT solution, 100 μL of DMSO was added to each well to solubilize formazan crystals generated by the viable cells. The absorbance was measured at 570 nm using a microplate reader (MTP-800; CORONA, Tokyo, Japan).

Apoptosis assay

After treatment, cell apoptosis was assessed by flow cytometry. Briefly, cells were washed in phosphate-buffered saline (PBS), fixed in 70% ethanol, and stained with propidium iodide (PI) and fluorescein isothiocyanate (FITC)-conjugated Annexin V in the presence of 50 μg/mL RNase A (Sigma-Aldrich). After incubating for 1 h at room temperature in the dark, the percentage of apoptotic cells was detected by FACScan (Beckman Coulter, Fullerton, CA, USA), followed by analysis using FlowJo software.

Measurement of cytochrome C release

The mitochondrial and cytosolic fractions from the cells were isolated using a Mitochondrial Fractionation Kit (Active Motif, Inc., Carlsbad, CA, USA). Briefly, ARPE-19 cells were seeded at a density of 2.4×10^5 cells/well in 6-well plates after treatment. After centrifugation at 600×g for 5 min, the cell pellet was resuspended in ice-cold 1× cytosolic buffer and incubated on ice for 15 min. After centrifugation at 800×g for 20 min, the supernatant was spun at 10,000×g for 20 min to collect the mitochondrial pellet. Subsequently, the mitochondrial fraction was collected by adding complete mitochondria buffer into mitochondrial pellet followed by incubation on ice for 15 min. The supernatant (cytosolic fraction) was obtained by centrifuging the supernatant at 16,000×g for 25 min. After isolating the mitochondrial and cytosolic fraction, the level of cytochrome C was detected using the Cytochrome C ELISA Kit (Abcam plc., Cambridge, MA, USA) following the manufacturer's instructions.

Caspase-3 activity assay

The cells were seeded into 6-well plates at a density of 2.4×10^5 cells/well after the treatment. Caspase-3-like protease activity in the lysate was detected using a colorimetric Caspase-3 Assay Kit (Sigma-Aldrich, Cat. No. CASP3C) following the manufacturer's instructions.

Real-time quantitative reverse transcription PCR (qRT-PCR)

Total RNA was isolated from cells using Trizol (Invitrogen) followed by reverse transcription using the Omniscript RT Kit (Qiagen, Hilden, Germany). qRT-PCR was performed using a standard SYBR Green PCR Kit (Toyobo, Osaka, Japan) in StepOnePlus™ (Applied Biosystems). The thermal profile included an initial denaturation for 20 s at 95°C, and quantification for 40 cycles of 3 s at 95°C and 30 s at 60°C. The levels of gene expression were calculated using the $2^{-\Delta\Delta CT}$ method with U6 and β-actin as the endogenous control genes for miRNA and RNA, respectively.

Luciferase reporter assay

In order to construct the reporter vectors VEGF-wild type (VEGF-WT) and VEGF-mutated type (VEGF-MUT), fragments from VEGF containing the predicted miR-939 binding site or mutated miR-939 binding site were cloned into a pMIR Glo Dual-luciferase miRNA Target Expression Vector (Promega, Madison, WI, USA). Subsequently, the vectors and miR-939 mimics were cotransfected into cells and the luciferase activity was tested using the Dual-Luciferase Reporter Assay System (Promega, Madison, WI, USA).

Western blot

Total protein was extracted from cells using RIPA lysis buffer (Beyotime Biotechnology, Shanghai, China) supplemented with protease inhibitors (Roche, Guangzhou, China), and quantified using the BCA™ Protein Assay Kit (Pierce, Appleton, WI, USA). The protein extracts were subjected to a Bio-Rad Bis-Tris Gel System for western blot. Primary antibodies for β-actin, VEGF, Bax, Bcl-2, pro-Caspase-3, cleaved-Caspase-3, pro-Caspase-9, cleaved-Caspase-9, AKT, p-AKT, PI3K, and p-PI3K were prepared in 5% blocking buffer at a dilution of 1:1,000 and used to incubate the polyvinylidene difluoride (PVDF) membrane (Millipore, MA, USA) at 4°C overnight. Subsequently, the membranes were probed with secondary antibody marked by horseradish peroxidase for 1 h at room temperature. After rinsing, the membranes were transferred into the Bio-Rad ChemiDoc™ XRS System and covered with 200 μL Immobilon Western Chemiluminescent HRP Substrate (Millipore). The signals were captured and analyzed by the Image Lab™ Software (Bio-Rad, Shanghai, China).

Statistical analysis

Experiments were performed in duplicate and repeated at least three times. Data from multiple experiments are presented as mean ± SD. Statistical analyses were performed using GraphPad 6.0 statistical software. Statistical significance between the groups was analyzed by one-way ANOVA at $P < 0.05$.

Results

Increased HEIH expression in serum of patients with DR

In this study, three groups of participants were enrolled including healthy participants (HC),

T1D patients without DR (NDR), and T1D patients with DR (DR). There were 22 males and 14 females in the HC group with an average age of 43.23±6.34 years; 21 males and 15 females in the NDR group with an average age of 45.52±5.67 years; and 23 males and 11 females in the DR group with an average age of 44.73±6.78 years. There was no significant difference in the body mass index, systolic blood pressure, diastolic blood pressure, liver function, and kidney function among the three groups. Moreover, we found that the expression of HEIH was significantly increased in the NDR and DR groups compared to the HC group ($P < 0.05$, **Figure 1A**). HEIH expression in the DR group was much higher than that in the NDR group ($P < 0.05$, **Figure 1A**).

HG induces injury in ARPE-19 cells

In order to confirm whether the DR model was successfully established by treating ARPE-19 cells with HG, we detected HG-induced injury in ARPE-19 cells. HG treatment significantly decreased cell viability ($P < 0.01$, **Figure 1B**), promoted apoptosis ($P < 0.001$, **Figure 1C**), increased cytochrome C release from mitochondria to cytoplasm ($P < 0.001$, **Figure 1D**), and enhanced caspase-3 activity ($P < 0.001$, **Figure 1E**) in ARPE-19 cells compared to control. Furthermore, we found that HG treatment distinctly induced the expression of HEIH in ARPE-19 cells ($P < 0.001$, **Figure 1F**).

Suppression of HEIH alleviates HG-induced ARPE-19 cell injury

In order to investigate the role of HEIH in DR, HEIH was overexpressed and suppressed by transfecting the cells with pcDNA-HEIH and si-HEIH, respectively. As shown in **Figure 2A**, HEIH expression was significantly increased in the pcDNA-HEIH group compared to the pcDNA3.1 group; however, the expression was distinctly decreased in the si-HEIH group compared to the si-NC group ($P < 0.001$, **Figure 2A**), indicating a high transfection efficiency. Moreover, the overexpression of HEIE significantly inhibited cell viability ($P < 0.05$, **Figure 2B**), induced apoptosis ($P < 0.01$, **Figure 2C** and **2D**), promoted cytochrome C release from mitochondria to cytoplasm ($P < 0.05$, **Figure 2E**), and enhanced caspase-3 activity ($P < 0.05$, **Figure 2F**) in ARPE-19 cells, whereas the suppression of HEIE had opposite effects ($P < 0.05$, **Figure 2B-F**).

HEIH regulates HG-induced ARPE-19 cell injury through miR-939

Accumulating evidence has revealed that lncRNAs could compete for endogenous RNAs (ceRNAs) to indirectly regulate mRNAs, thus playing crucial roles in the development of human diseases [15]. It has been reported that miR-939 expression is low in patients with diabetes mellitus [16]. Therefore, we investigated whether HEIH is involved in DR by regulating miR-939. The miR-939 expression was significantly decreased in the pcDNA-HEIH group compared to the pcDNA3.1 group; however, expression was significantly increased in the si-HEIH group compared to si-NC group ($P < 0.01$, **Figure 3A**), indicating that HEIH negatively regulates miR-939. We further overexpressed and suppressed miR-939 by transfecting the cells with miR-939 mimic and miR-939 inhibitor, respectively, and obtained a high transfection efficiency ($P < 0.001$, **Figure 3B**). Subsequently, the HG-treated ARPE-19 cells were cotransfected with si-HEIH and miR-939 inhibitor. The effects of HEIH suppression on the cell viability, apoptosis, cytochrome C release from mitochondria to cytoplasm, and caspase-3 activity were remarkably reversed by inhibiting miR-939 ($P < 0.05$, **Figure 3C-F**).

VEGF as a functional target of miR-939

VEGF has been reported to function as a survival factor in the retina in early DR [17]. Analysis using TargetScan revealed that VEGF is a potential target of miR-939. The binding sequences of miR-939 and VEGF are shown in **Figure 4A** (http://www.targetscan.org/cgi-bin/targetscan/vert_71/view_gene.cgi?rs=ENST00000372067.3&taxid=9606&members=miR-939-3p&showcnc=0&shownc=0&showncf1=1&showncf2=1&subset=1). Moreover, the luciferase activity of VEGF-WT was significantly inhibited by miR-939 ($P < 0.05$, **Figure 4B**). Furthermore, the mRNA and protein expression levels of VEGF were significantly decreased in miR-939 mimic group and remarkably increased in the miR-939 inhibitor group compared to the corresponding controls ($P < 0.01$, **Figure 4C** and **4D**).

miR-939 regulates HG-induced ARPE-19 cell injury through VEGF

In order to further verify whether miR-939 regulates HG-induced ARPE-19 cell injury through

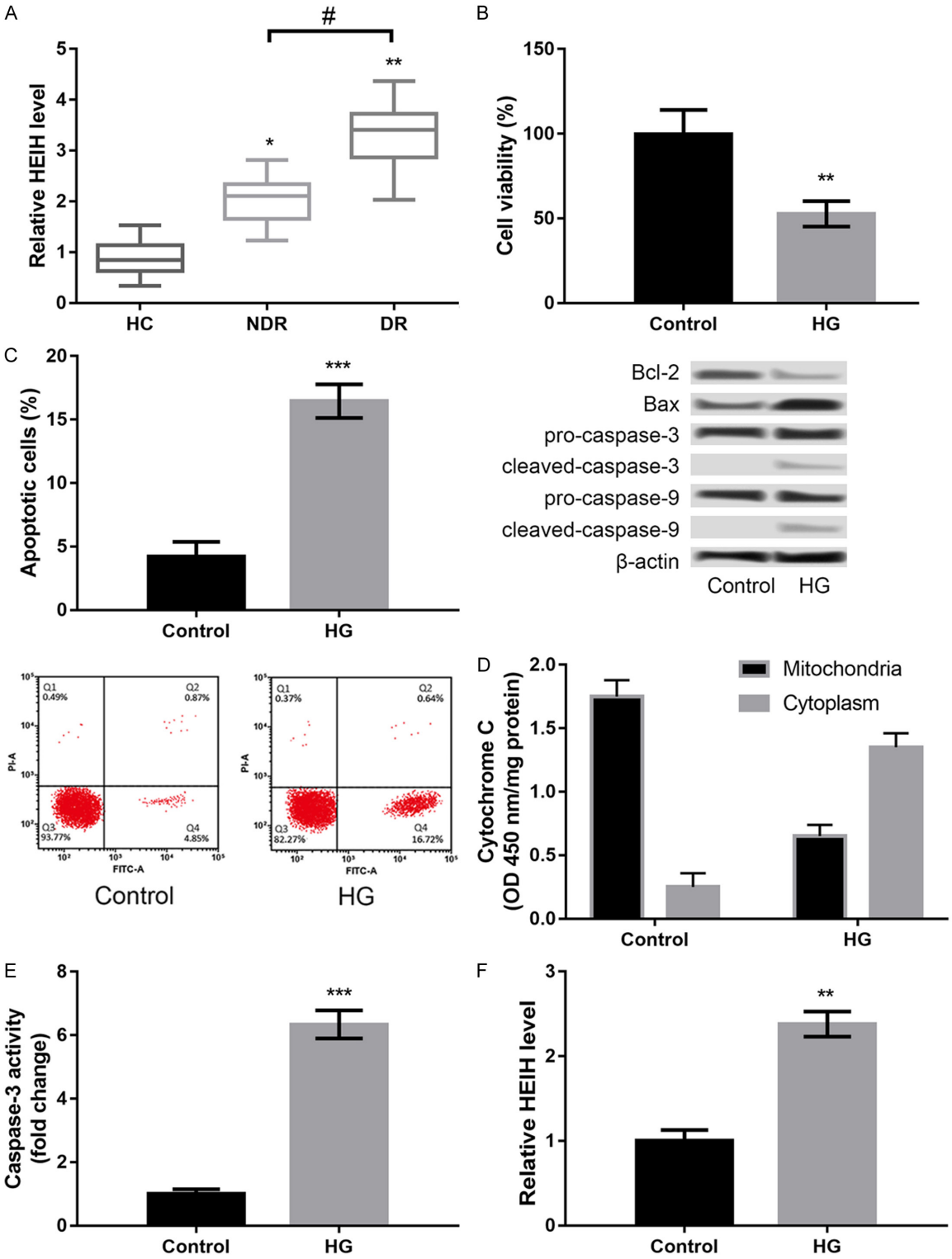

Figure 1. LncRNA HEIH was highly expressed in serum samples of patients with diabetic retinopathy (DR) (A) and high concentrations of D-glucose (HG) induced injury in APRE-19 cells. *P < 0.05 and **P < 0.01 compared with healthy controls (HC). #P < 0.05 compared with type 1 diabetes (T1D) patients without DR (NDR group). (B) Cell viability after HG treatment. (C) Cell apoptosis after HG treatment and the expression levels of apoptosis-related proteins. (D) Cytochrome C release from mitochondria to cytoplasm after HG treatment. (E) Caspase-3 activity after HG treatment. (F) The expression levels of HEIH after HG treatment. All experiments were repeated three times and the data are presented as the mean ± SD. **P < 0.01, and ***P < 0.001 compared to controls.

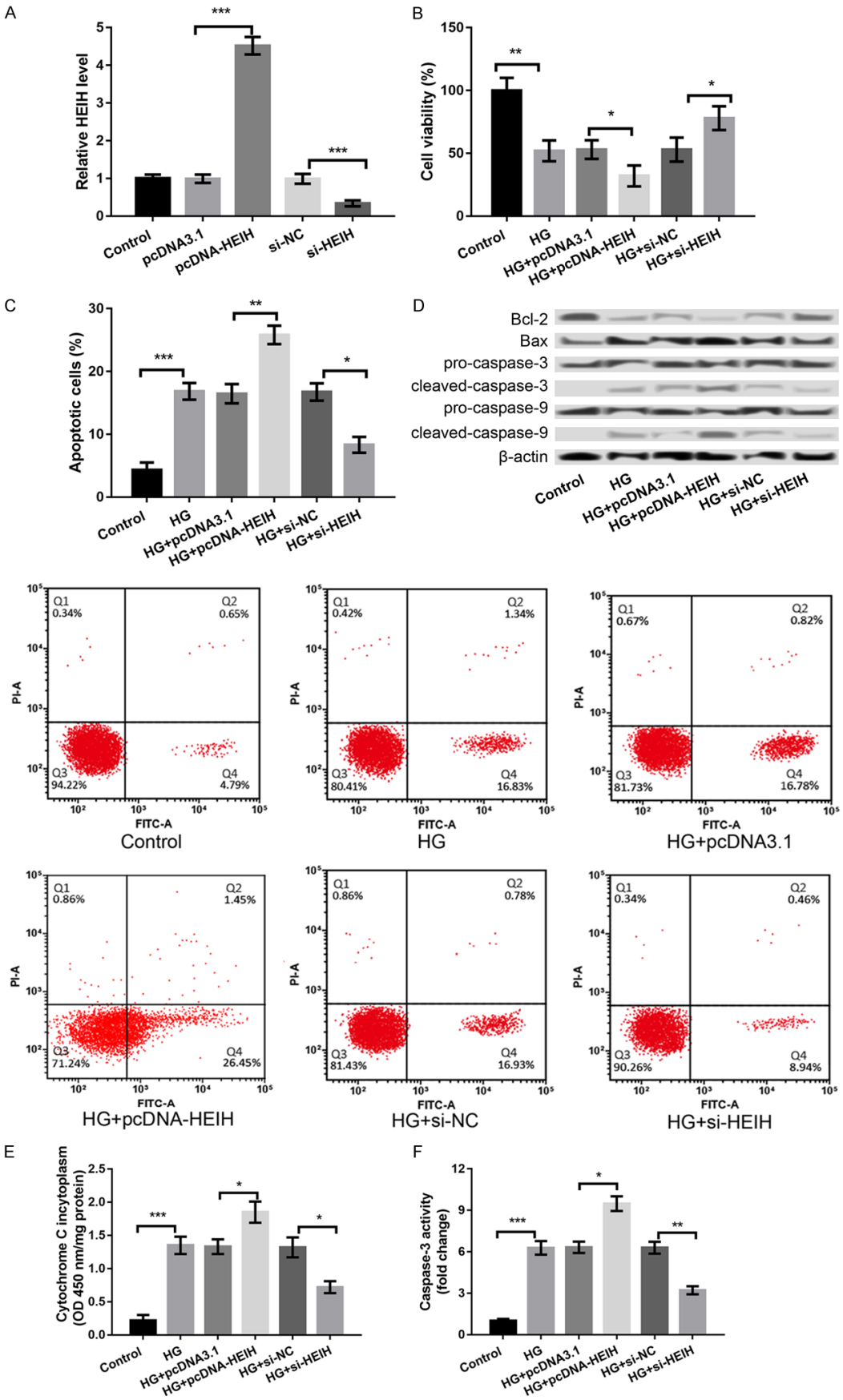
A
Relative HEIH level
Control
pcDNA3.1
pcDNA-HEIH
si-NC
si-HEIH
B
Cell viability (%)
Control
HG
HG+pcDNA3.1
HG+pcDNA-HEIH
HG+si-NC
HG+si-HEIH
C
Apoptotic cells (%)
D
Bcl-2
Bax
pro-caspase-3
cleaved-caspase-3
pro-caspase-9
cleaved-caspase-9
β-actin
Q1 0.34%
Q2 0.65%
Q3 94.22%
Q4 4.79%
Control
Q1 0.42%
Q2 1.34%
Q3 80.41%
Q4 16.83%
HG
Q1 0.67%
Q2 0.82%
Q3 81.73%
Q4 16.78%
HG+pcDNA3.1
Q1 0.86%
Q2 1.45%
Q3 71.24%
Q4 26.45%
HG+pcDNA-HEIH
Q1 0.86%
Q2 0.78%
Q3 81.43%
Q4 16.93%
HG+si-NC
Q1 0.34%
Q2 0.46%
Q3 90.26%
Q4 8.94%
HG+si-HEIH
PI-A
FITC-A
E
Cytochrome C incytoplasm (OD 450 nm/mg protein)
F
Caspase-3 activity (fold change)

Figure 2. The overexpression of HEIH aggravated HG-induced APRE-19 cell injury, whereas the suppression of HEIH alleviated this injury. A: HEIH expression after transfection with pcDNA-HEIH, si-HEIH, and respective controls. B: Cell viability in the treated groups. C: Cell apoptosis in the treated groups. D: Expression levels of apoptosis-related proteins in the treated groups. E: Cytochrome C release from mitochondria to cytoplasm in the treated groups. F: Caspase-3 activity in the treated groups. All experiments were repeated three times and the data are presented as the mean ± SD. *P < 0.05, **P < 0.01, ***P < 0.001 compared with corresponding controls.

VEGF, VEGF was overexpressed and knocked down in ARPE-19 cells. We analyzed the combined effects of miR-939 overexpression and VEGF overexpression on HG-induced ARPE-19 cell injury. As presented in **Figure 5A**, the VEGF expression was significantly increased in the pEX-VEGF group compared to the pEX group (P < 0.001) and significantly decreased in sh-VEGF group compared to sh-NC group (P < 0.001). Subsequent experiments revealed that the overexpression of miR-939 alleviated HG-induced ARPE-19 cell injury by promoting cell viability (P < 0.05, **Figure 5B**), inhibiting apoptosis (P < 0.01, **Figure 5C**), decreasing cytochrome C release from mitochondria to cytoplasm (P < 0.01, **Figure 5D**), and repressing caspase-3 activity (P < 0.01, **Figure 5E**). Further experiments disclosed that the overexpression of miR-939 and VEGF at the same time reversed the effects of overexpression of miR-939 alone on HG-induced ARPE-19 cell injury (P < 0.01, **Figure 5B-E**), indicating that miR-939 regulated HG-induced ARPE-19 cell injury by modulating VEGF.

PI3K/AKT pathway as a possible downstream mechanism of HEIH/miR-939/VEGF axis in regulating HG-induced ARPE-19 cell injury

PI3K/AKT signaling pathway is one of the pathways activated by VEGF, which plays a key role in regulating cell proliferation, apoptosis, and migration [18, 19]. The PI3K/AKT/mTOR pathway was reported to be involved in the pathophysiology of DR [20]. Therefore, we investigated a regulatory role of the HEIH/miR-939/VEGF axis in the activation of PI3K/AKT signaling pathway. As shown in **Figure 5F**, HG treatment increased the expression of p/t-PI3K and p/t-AKT, indicating that HG promoted the activation of PI3K/AKT signaling pathway, which was reversed by the suppression of HEIH (P < 0.05, **Figure 5F**). Moreover, the effects of the suppression of HEIH on HG-induced activation of PI3K/AKT signaling pathway was reversed by inhibiting miR-939 concurrently, which was further reversed by synchronous knockdown of VEGF (P < 0.05, **Figure 5F**).

Discussion

Identification of key lncRNAs involved in DR will provide new insight into the diagnosis and treatment of this disease. Previous studies have shown that lncRNA HEIH promotes the development of colorectal cancer [14] and hepatitis C virus (HCV)-related hepatocellular carcinoma [21]. In this study, we found that HEIH is highly expressed in the serum of patients with DR. Moreover, HG induced ARPE-19 cell injury and promoted the expression of HEIH. Overexpression of HEIE aggravated HG-induced ARPE-19 cell injury by significantly inhibiting cell viability, inducing apoptosis, promoting cytochrome C release from mitochondria to cytoplasm, and enhancing the caspase-3 activity, whereas the suppression of HEIE had opposite effects. These results indicated that HEIH may promote DR development.

Moreover, our results showed that miR-939 was negatively regulated by HEIH. Earlier studies have reported that miR-939 plays a key role in the development and progression of several cancers, such as gastric cancer [22], ovarian cancer [23], and colorectal cancer [14]. Although miR-939 is reported to be expressed at low levels in patients with diabetes mellitus [16], the key role of miR-939 in DR has not been fully investigated. In this study, we found that the effects of the suppression of HEIH on HG-induced ARPE-19 cell injury were strongly reversed by inhibiting miR-939. These findings indicated that miR-939 might be a downstream target of HEIH and plays a key role in DR development.

miRNAs play regulatory roles in fundamental biologic processes by negatively regulating their target genes at the posttranscriptional level. In this study, VEGF was identified as a target of miR-939. A previous study has shown VEGF as a survival factor in ex vivo models of early DR [17]. Moreover, a polymorphism of HMGA1 (rs139876191 variant) plays a protective role against proliferative DR by suppressing HMGA1-induced VEGFA expression [24]. miR-

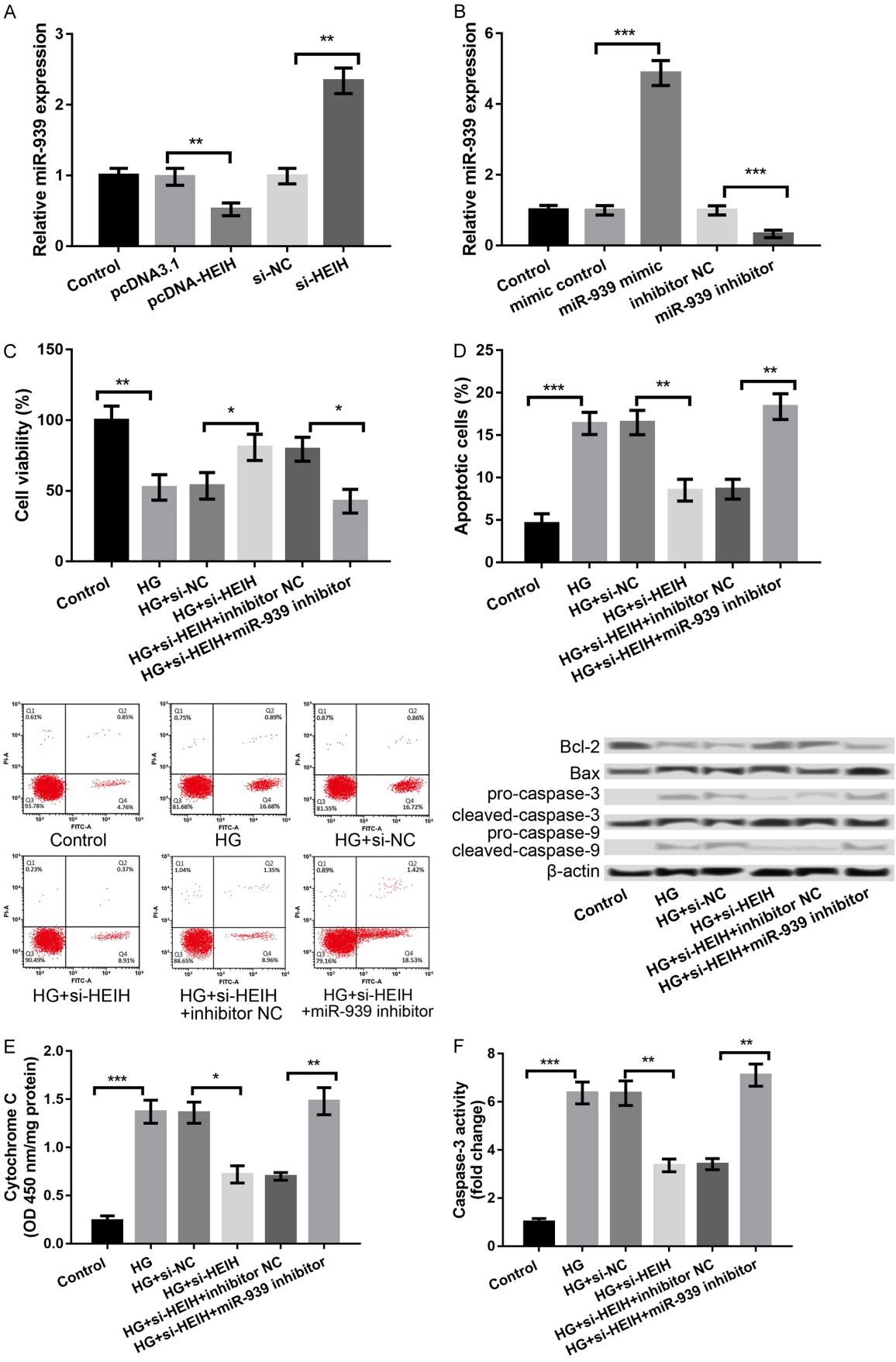
A
Relative miR-939 expression
Control
pcDNA3.1
pcDNA-HEIH
si-NC
si-HEIH
B
Relative miR-939 expression
Control
mimic control
miR-939 mimic
inhibitor NC
miR-939 inhibitor
C
Cell viability (%)
Control
HG
HG+si-NC
HG+si-HEIH
HG+si-HEIH+inhibitor NC
HG+si-HEIH+miR-939 inhibitor
D
Apoptotic cells (%)
Control
HG
HG+si-NC
HG+si-HEIH
HG+si-HEIH+inhibitor NC
HG+si-HEIH+miR-939 inhibitor
Control
HG
HG+si-NC
HG+si-HEIH
HG+si-HEIH +inhibitor NC
HG+si-HEIH +miR-939 inhibitor
Bcl-2
Bax
pro-caspase-3
cleaved-caspase-3
pro-caspase-9
cleaved-caspase-9
β-actin
Control
HG
HG+si-NC
HG+si-HEIH
HG+si-HEIH+inhibitor NC
HG+si-HEIH+miR-939 inhibitor
E
Cytochrome C (OD 450 nm/mg protein)
Control
HG
HG+si-NC
HG+si-HEIH
HG+si-HEIH+inhibitor NC
HG+si-HEIH+miR-939 inhibitor
F
Caspase-3 activity (fold change)
Control
HG
HG+si-NC
HG+si-HEIH
HG+si-HEIH+inhibitor NC
HG+si-HEIH+miR-939 inhibitor

Figure 3. HEIH regulated HG-induced APRE-19 cell injury through negative regulation of miR-939. A: miR-939 expression after transfection with pcDNA-HEIH, si-HEIH, and respective controls. B: miR-939 expression after transfection with miR-939 mimic, miR-939 inhibitor, and their controls. C: Cell viability in the treated groups. D: Cell apoptosis in the treated groups and the expression levels of apoptosis-related proteins. E: Cytochrome C release from mitochondria to cytoplasm in the treated groups. F: Caspase-3 activity in the treated groups. All experiments were repeated three times and the data are presented as the mean ± SD. *P < 0.05, **P < 0.01, ***P < 0.001 compared with corresponding controls.

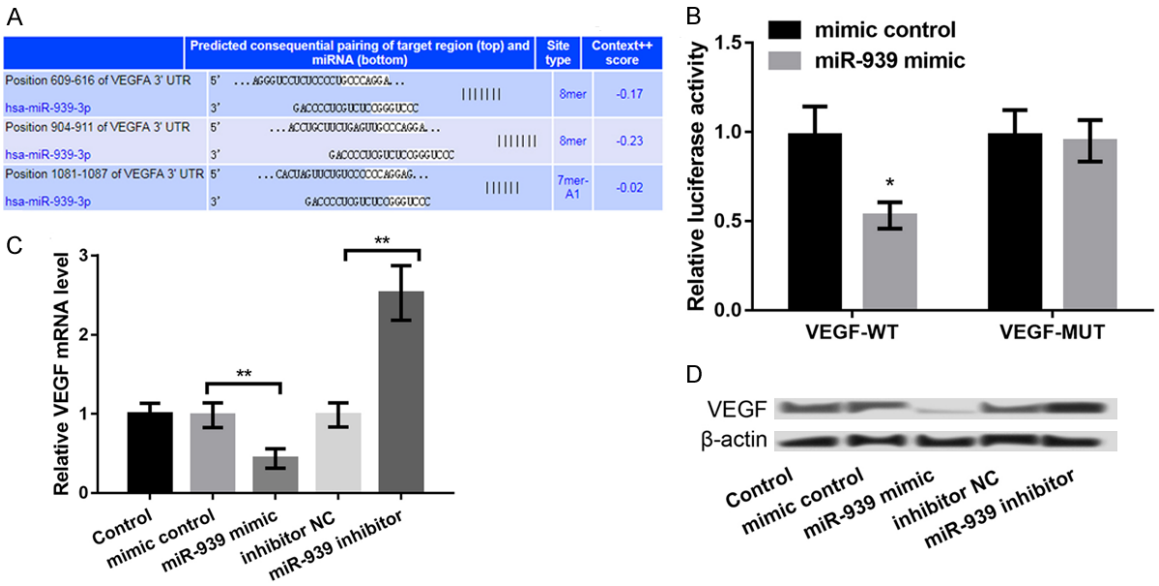

Figure 4. VEGF as a target of miR-939. A: Predicted binding sequence between VEGFA and miR-939. B: Luciferase reporter assay showing that miR-939 could interact with VEGF-WT. C and D: The expression levels of VEGF mRNA and protein after transfection with miR-939 mimic, miR-939 inhibitor, and their controls. All experiments were repeated three times and the data are expressed as the mean ± SD. *P < 0.05, and **P < 0.01, ***P < 0.001 compared to respective controls.

200b alleviates the development of DR by targeting VEGFA [25]. These studies suggested a key role of VEGF in DR. In this study, we found that miR-939 regulated HG-induced ARPE-19 cell injury through VEGF. Therefore, we speculate that miR-939 may aggravate DR by targeting VEGF.

Furthermore, VEGF activates PI3K/AKT signaling pathway, which plays an important role in regulating cell proliferation, apoptosis, and migration [18, 19]. It was reported that Nogo-B, a conserved protein of endoplasmic reticulum, promotes angiogenesis in proliferative DR through the VEGF/PI3K/AKT pathway [26]. Our results showed that the suppression of HEIH inhibited HG-induced activation of the PI3K/AKT signaling pathway. Moreover, the effect of the suppression of HEIH on HG-induced activation of the PI3K/AKT signaling pathway was reversed by the inhibition of miR-939 concurrently, which was further reversed by synchronous knockdown of VEGF. It can, therefore, be speculated that the PI3K/AKT pathway is a possible downstream mechanism of HEIH/miR-939/VEGF axis in regulating HG-induced ARPE-19 cell injury, and the PI3K/AKT pathway may mediate the role of HEIH in DR development.

In conclusion, our findings revealed that HEIH may contribute to DR by sponging miR-939 to target VEGF expression and by regulating activation of the PI3K/AKT pathway. HEIH/miR-939/VEGF axis may provide a novel perspective for DR therapy.

Disclosure of conflict of interest

None.

Address correspondence to: Chengyuan Zhao, Department of Endocrinology, Taizhou People's Hospital, 366 Taihu Road, Taizhou Medical High-te-

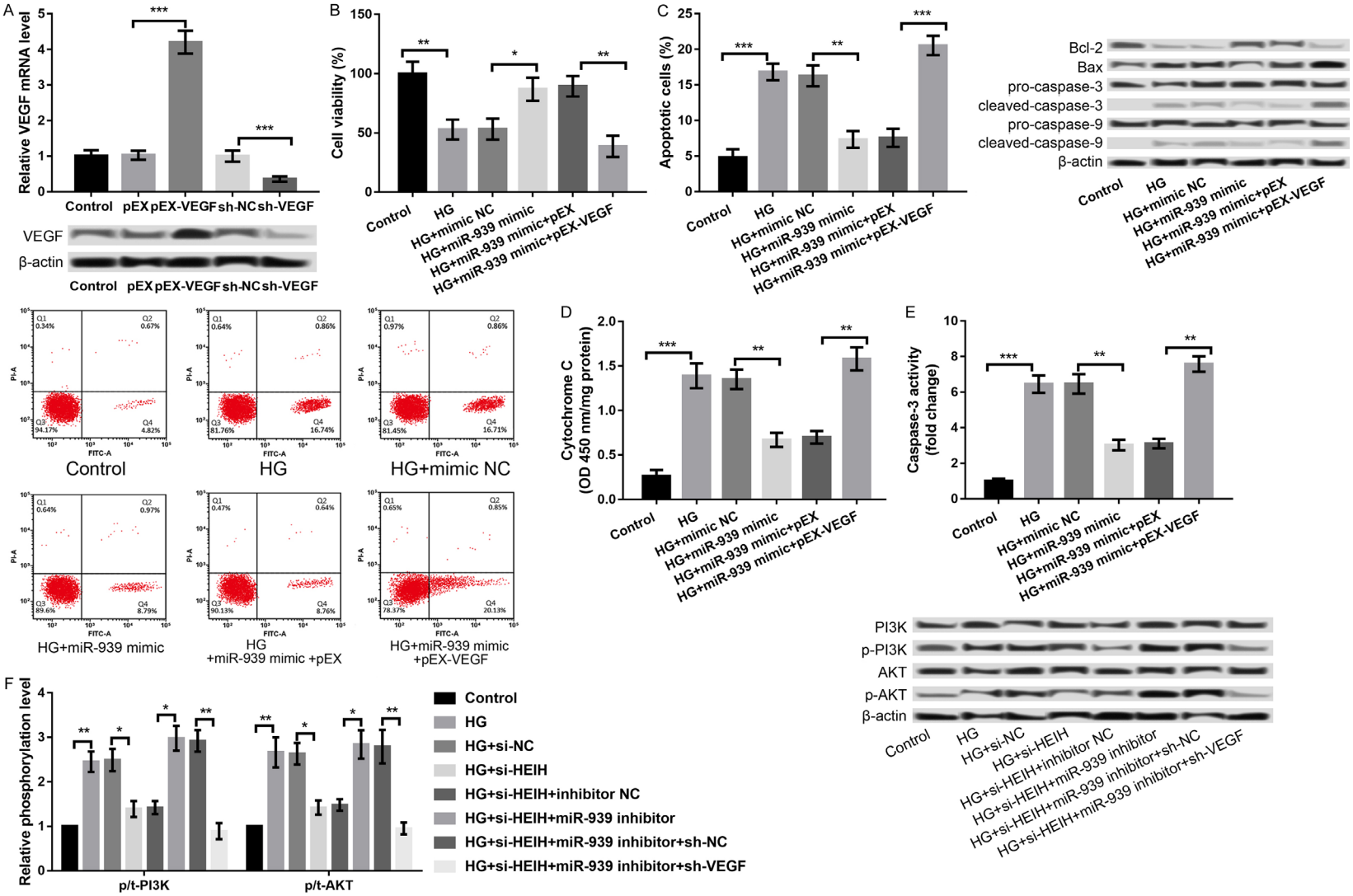

Figure 5. miR-939 regulated HG-induced APRE-19 cell injury through targeting VEGF. A: The mRNA and protein expression of VEGF after transfection with pEX-VEGF, sh-VEGF, and their controls. B: Cell viability in the treated groups. C: Cell apoptosis in the treated groups and the expression levels of apoptosis-related proteins. D: Cytochrome C release form mitochondria to cytoplasm in the treated groups. E: Caspase-3 activity in the treated groups. F: The regulatory effects of HEIH/miR-939/VEGF axis on protein expression of PI3K/AKT signaling pathway-related proteins in the HG-treated APRE-19 cells. All experiments were repeated three times and the data are presented as the mean ± SD. *P < 0.05, **P < 0.01, ***P < 0.001 compared to corresponding controls.

ch Zone, Taizhou 225300, Jiangsu, China. E-mail: chengyuanzhao06@163.com

References

[1] Ravindran R, Gopinathan DM and Sukumaran S. Estimation of salivary glucose and glycogen content in exfoliated buccal mucosal cells of patients with type II diabetes mellitus. J Clin Diagn Res 2015; 9: ZC89-93.

[2] Wild S, Roglic G, Green A, Sicree R and King H. Global prevalence of diabetes estimates for the year 2000 and projections for 2030. Diabetes Care 2004; 27: 1047-1053.

[3] Hammes HP, Feng Y, Pfister F and Brownlee M. Diabetic retinopathy: targeting vasoregression. Diabetes 2011; 60: 9-16.

[4] Leasher JL, Bourne RR, Flaxman SR, Jonas JB, Keeffe J, Naidoo K, Pesudovs K, Price H, White RA and Wong TY. Global estimates on the number of people blind or visually impaired by diabetic retinopathy: a meta-analysis from 1990 to 2010. Diabetes Care 2016; 39: 1643-1649.

[5] Armulik A, Abramsson A and Betsholtz C. Endothelial/pericyte interactions. Circ Res 2005; 97: 512-523.

[6] Tapp RJ, Shaw JE, Harper CA, de Courten MP, Balkau B, Mccarty DJ, Taylor H, Welborn TA, Zimmet PZ; AusDiab Study Group. The prevalence of and factors associated with diabetic retinopathy in the Australian population. Diabetes Care 2003; 26: 1731-1737.

[7] Clemson CM, Hutchinson JN, Sara SA, Ensminger AW, Fox AH, Chess A and Lawrence JB. An architectural role for a nuclear noncoding RNA: NEAT1 RNA is essential for the structure of paraspeckles. Mol Cell 2009; 33: 717-726.

[8] Res C. Correction: long noncoding RNA HOTAIR regulates polycomb-dependent chromatin modification and is associated with poor prognosis in colorectal cancers. Cancer Res 2011; 71: 6320-6326.

[9] Beltran M, Puig I, Peña C, García JM, Álvarez AB, Peña R, Bonilla F and de Herreros AG. A natural antisense transcript regulates Zeb2/Sip1 gene expression during Snail1-induced epithelial-mesenchymal transition. Genes Dev 2008; 22: 756-769.

[10] Thomas AA, Biswas S, Feng B, Chen S, Gonder J and Chakrabarti S. lncRNA H19 prevents endothelial-mesenchymal transition in diabetic retinopathy. Diabetologia 2019; 62: 517-530.

[11] Zhang D, Qin H, Leng Y, Li X, Zhang L, Bai D, Meng Y, Wang J. LncRNA MEG3 overexpression inhibits the development of diabetic retinopathy by regulating TGF-β1 and VEGF. Exp Ther Med 2018; 16: 2337-2342.

[12] Li XJ. Long non-coding RNA nuclear paraspeckle assembly transcript 1 inhibits the apoptosis of retina Müller cells after diabetic retinopathy through regulating miR-497/brain-derived neurotrophic factor axis. Diab Vasc Dis Res 2018; 15: 204-213.

[13] Yang F, Zhang L, Huo XS, Yuan JH, Xu D, Yuan SX, Zhu N, Zhou WP, Yang GS and Wang YZ. Long noncoding RNA high expression in hepatocellular carcinoma facilitates tumor growth through enhancer of zeste homolog 2 in humans. Hepatology 2011; 54: 1679-1689.

[14] Cui C, Zhai D, Cai L, Duan Q, Xie L and Yu J. Long noncoding RNA HEIH promotes colorectal cancer tumorigenesis via counteracting miR-939-mediated transcriptional repression of Bcl-xL. Cancer Res Treat 2018; 50: 992-1008.

[15] Zhang G, Sun H, Zhang Y, Zhao H, Fan W, Li J, Lv Y, Song Q and Zhang M. Characterization of dysregulated lncRNA-mRNA network based on ceRNA hypothesis to reveal the occurrence and recurrence of myocardial infarction. Cell Death Discov 2018; 4: 35.

[16] Collares CV, Evangelista AF, Xavier DJ, Rassi DM, Arns T, Foss-Freitas MC, Foss MC, Puthier D, Sakamoto-Hojo ET and Passos GA. Identifying common and specific microRNAs expressed in peripheral blood mononuclear cell of type 1, type 2, and gestational diabetes mellitus patients. BMC Res Notes 2013; 6: 491.

[17] Amato R, Biagioni M, Cammalleri M, Dal MM and Casini G. VEGF as a survival factor in Ex vivo models of early diabetic retinopathy. Invest Ophthalmol Vis Sci 2016; 57: 3066-3076.

[18] Nakashio A, Fujita N and Tsuruo T. Topotecan inhibits VEGF- and bFGF-induced vascular endothelial cell migration via downregulation of the PI3K-Akt signaling pathway. Int J Cancer 2002; 98: 36-41.

[19] Ashida M. Inhibition of epidermal growth factor receptor and PI3K/Akt signaling suppresses cell proliferation and survival through regulation of Stat3 activation in human cutaneous squamous cell carcinoma. J Skin Cancer 2011; 2011: 874571.

[20] Jacot JL and Sherris D. Potential therapeutic roles for inhibition of the PI3K/Akt/mTOR pathway in the pathophysiology of diabetic retinopathy. J Ophthalmol 2011; 2011: 589813.

[21] Zhang C, Yang X, Qi Q, Gao Y, Wei Q and Han S. lncRNA-HEIH in serum and exosomes as a potential biomarker in the HCV-related hepatocellular carcinoma. Cancer Biomark 2018; 21: 651-659.

[22] Zhang JX, Xu Y, Gao Y, Chen C, Zheng ZS, Yun M, Weng HW, Xie D and Ye S. Decreased expression of miR-939 contributes to chemoresistance and metastasis of gastric cancer via dysregulation of SLC34A2 and Raf/MEK/ERK pathway. Mol Cancer 2017; 16: 18.

[23] Ying X, Li-ya Q, Feng Z, Yin W and Ji-hong L. MiR-939 promotes the proliferation of human ovarian cancer cells by repressing APC2 ex-

pression. Biomed Pharmacother 2015; 71: 64-69.
[24] Chiefari E, Ventura V, Capula C, Randazzo G, Scorcia V, Fedele M, Arcidiacono B, Nevolo MT, Bilotta FL and Vitiello M. A polymorphism of HMGA1 protects against proliferative diabetic retinopathy by impairing HMGA1-induced VEGFA expression. Sci Rep 2016; 6: 39429.
[25] Li EH, Huang QZ, Li GC, Xiang ZY and Zhang X. Effects of microRNA-200b on the development of diabetic retinopathy by targeting VEGFA gene. Biosci Rep 2017; 37.
[26] Zhang Y, Wang L, Wang M, Sun Q, Xia F, Wang R and Liu L. Nogo-B promotes angiogenesis in proliferative diabetic retinopathy via VEGF/PI3K/Akt pathway in an autocrine manner. Cell Physiol Biochem 2017; 43: 1742-1754.